Supporting Information

One Ligand, Two Roles: Novel Pillar-Layer Metal-Organic Frameworks

Built with a 3D ligand and Asymmetric Inorganic Nodes

Chaozhuang Xue[+],*[a] Yingying Zhang[+],[b] Kai Zhu,[b] Suyun Deng,[b] Konggang Qu,[a] Shuwen Gong,*[a] and Huajun Yang*[b]

[a]*Dr. C. Xue, Dr. K. Qu, Prof. S. Gong, School of Chemistry and Chemical Engineering, Liaocheng University, Liaocheng 252059, China. E-mail: czxuelc@163.com, gongshw@lcu.edu.cn*
[b]*Y. Zhang, K. Zhu, S. Deng, Prof. H. Yang, Jiangsu Key Laboratory of Biomedical Materials, School of Chemistry and Materials Science, Nanjing Normal University, Nanjing 210023, China. E-mail:*   *huajunyang@nnu.edu.cn*

Experimental section

Synthesis of compound 1: Co(NO$_3$)$_2$·6H$_2$O (87 mg, ~0.3 mmol), bcp (47 mg, 0.3 mmol) and anhydrous DMF (2.7 mL) were added in 15 mL glass vial and then ultrasonically treated for 10 min to obtain clear solution. The vial was sealed and placed in 130 °C oven for 12 h. Purple prismatic or platelike compound 1 crystals were obtained after cooling to room temperature. The yield was about 65 % based on the Co (Experimental: ~40 mg; Theoretical: 59.4 mg). The phase purity was verified by the powder X-ray diffraction. The obtained sample was soaked in DMF for 24 h, for the subsequent measurements.

Synthesis of compound 2: Co(NO$_3$)$_2$·6H$_2$O (87 mg, ~0.3 mmol), bcp (47 mg, 0.3 mmol) and NMF (3 mL) were added in 15 mL glass vial and then ultrasonically treated for 10 min to obtain clear solution. The vial was sealed and placed in 130 °C oven for three days. Purple prismatic compound 2 crystals were obtained after cooling to room temperature. The yield was about 50 % based on the Co (Experimental: ~30 mg; Theoretical: 59.2 mg). The phase purity was verified by the powder X-ray diffraction. The obtained sample was soaked in DMF for 24 h, for the subsequent measurements.

Structural characterizations: Single-crystal X-ray diffraction (SCXRD) data for both two compounds were collected using Bruker CCD diffractometer with graphite-monochromated Mo-Kα (λ = 0.71073 Å) radiation at room temperature. Absorption corrections on two compounds were performed using the multi-scan program in APEX3. The structure was solved by a direct method using SHELXS-2014, and refinement against all reflections of the compounds was performed using SHELXL-2014. Solvent molecules were removed from the data set using the SQUEEZE routine of PLATON and refined further using the data generated. Powder X-ray Diffraction (PXRD) measurements on as-synthesized samples by using a Rigaku SmartLab X-ray powder diffractometer with Cu-Kα radiation. The data collection performed at room temperature in the range from 3° to 30° with a step size of ~0.01°, speed duration time of 10, IS of 1/2 deg, RS1 of 20 mm. Thermogravimetric (TGA) analysis was carried out on a Netzch STA449F3 analyzer heated from ambient temperature to 800 °C under a nitrogen gas atmosphere with a heating rate of 25 °C/min. Fourier transform infrared spectroscopy (FTIR) was recorded on a Brucker Tensor 27 in the range of 4000-400 cm^{-1} using the KBr pellets. Elemental analysis (EA) was performed on VARIDEL III elemental analyzer in C/H/N/S mode and O mode respectively, to determine the contents of carbon,

hydrogen, nitrogen, as well as oxygen.

Gas adsorption measurements: N_2 adsorption measurements were carried out on Automatic High Performance Surface Area and Aperture Analyzer (BSD-660 A3M). Single-component Xe and Kr adsorption isotherms at 273 K and 298 K were performed by using a Micromeritics ASAP 2020Plus adsorption apparatus. Ultrahigh purity grade N_2 (99.999 %), Kr (99.999%) and Xe (99.999%) were applied for all measurements. Prior to the measurement, the samples were washed with dichloromethane for 3 times and soaked in dichloromethane for three days. During each day, the solution was refreshed. After solvent exchange, the upper solvent was decanted. The sample was first dried under N_2 flow gently and was subsequently transferred into the test tube. The degas program was set as heating to 100 °C, then keeping 100 °C for 6 h in situ degassing.

Xe and Kr breakthrough measurements: Experimental column breakthrough measurements were conducted by using a Multi-constituent Adsorption Breakthrough Curve Analyzer (BSD-MAB) on a 7.5 cm long and 0.6 cm diameter column packed with solve-exchanged compound 1 sample. The sample was degassed at 100 °C for 6 hours. After flowing pure He gas for three minutes, the Xe/Kr gas mixture (20/80, v/v) was introduced to the fixed bed column with a total flowing rate of 2 mL min^{-1} at 298 K and 1 bar.

Isosteric Heat of Adsorption (Qst): The isosteric heats of adsorption for all the gases were calculated using the isotherms at 273 K and 298 K, following the Clausius-Clapeyron equation. It was done with the calculation program embedded in the software of Automatic High Performance Surface Area and Aperture Analyzer (ASAP 2020Plus). High accuracy of the Qst was found in all the calculations as evidenced by the linearity in the isosters.

Selectivity by IAST. To evaluate the Xe/Kr separation performance, the selectivity was calculated by ideal adsorbed solution theory (IAST). Dual-Site Langmuir-Freundlich (DSLF) model was employed to fit the gas adsorption isotherms over the entire pressure range. DSLF model can be written as:

$$N = \frac{A_1 B_1 P^{1/n_1}}{1 + B_1 P^{1/n_1}} + \frac{A_2 B_2 P^{1/n_2}}{1 + B_2 P^{1/n_2}} \tag{1}$$

Where N is the quantity adsorbed, p is the pressure of bulk gas at equilibrium with adsorbed phase, A_i is the saturation loadings for adsorption site i (i=1 or 2), and B_i are the affinity parameters. $1/n_i$ is the index of heterogeneity. The R factors for all the fitting are close to or higher than 99.999%.

The detailed methodology for calculating the amount of A and B adsorption from a mixture by IAST is described elsewhere. The adsorption selectivity is finally defined as:

$$selectivity = \frac{q_A / q_B}{p_A / p_B} \qquad (2)$$

where q_i (i = A or B) is the uptake quantity in the mixture and p_i is the feeding partial pressure of component i.
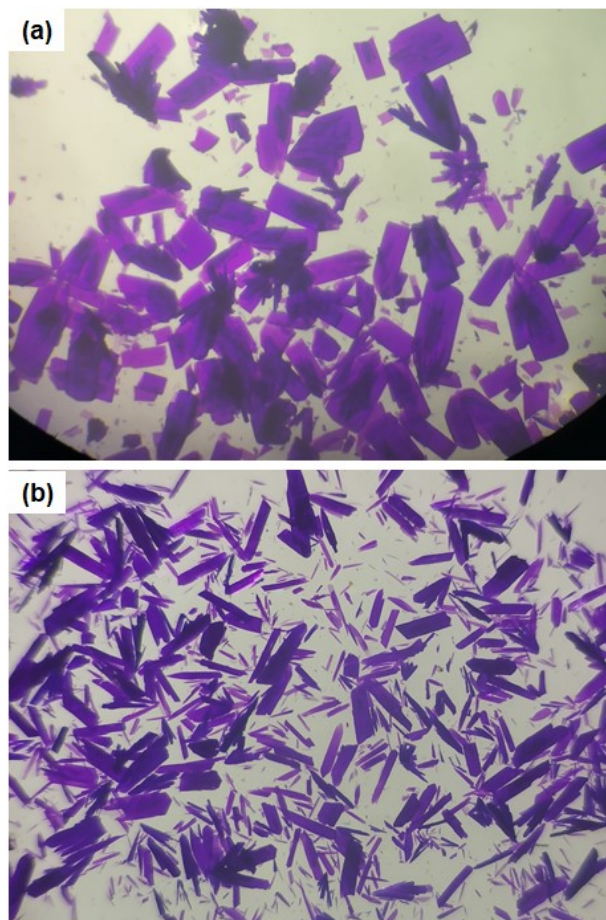
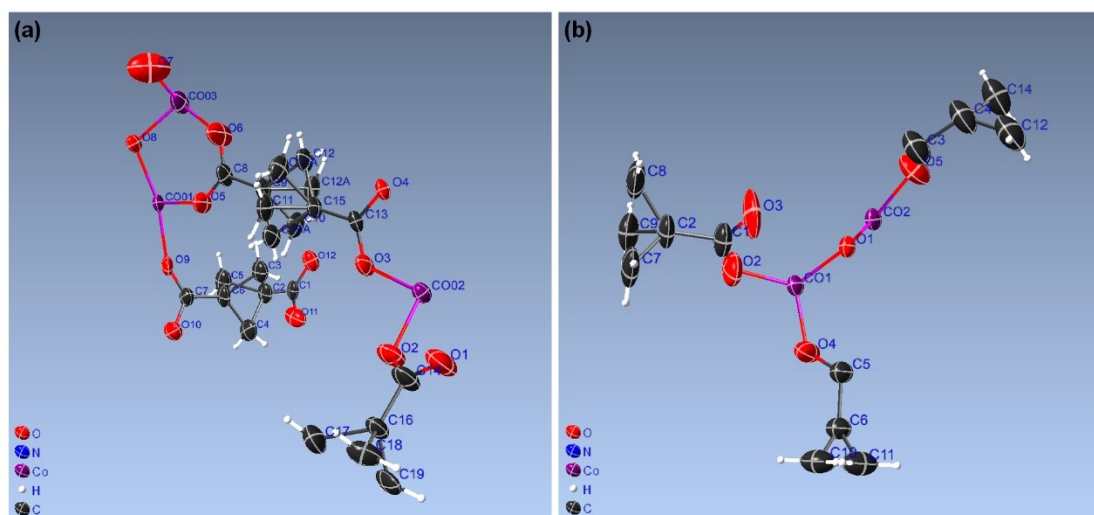**Fig. S1** Optical pictures for compound 1 (a) and 2 (b).
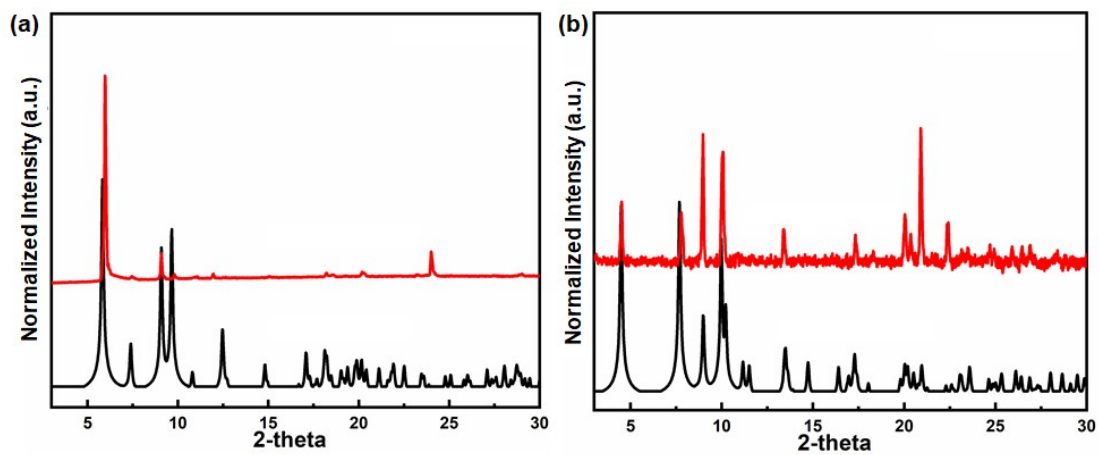

Fig. S2 The asymmetric units in compound 1 and compound 2.

Fig. S3 PXRD patterns for compound 1 (a) and 2 (b). black: simulated; red: experimental
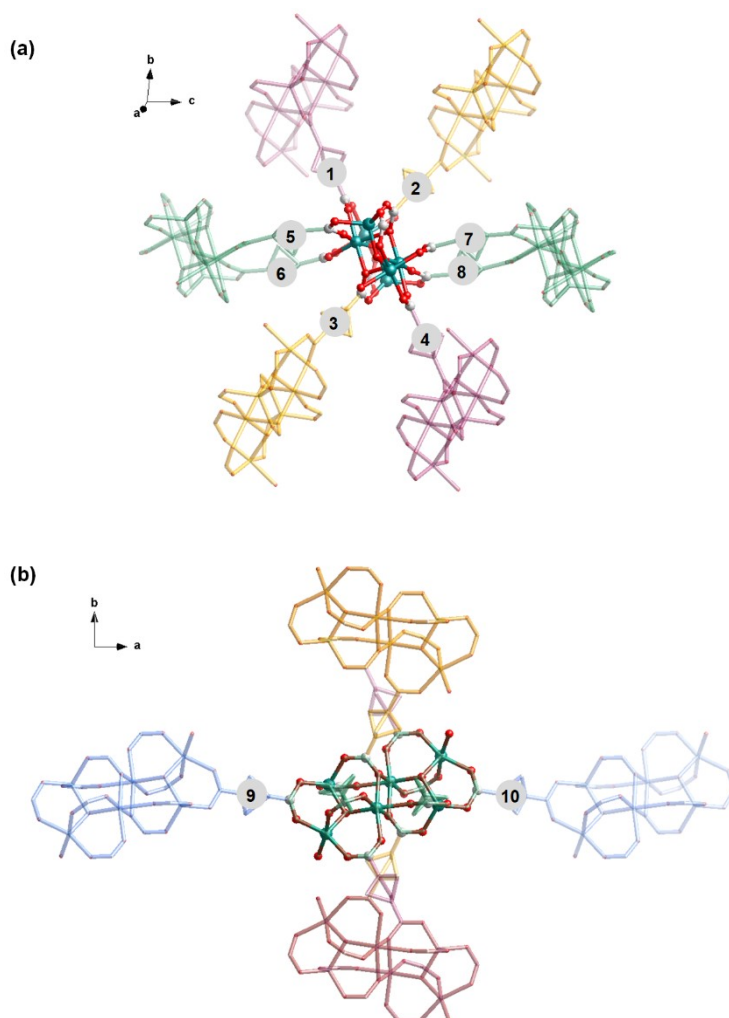

Fig. S4 10-*c* inorganic cluster node in compound 1. (a) eight intralayer extending sites. (b) two interlayer extending sites.
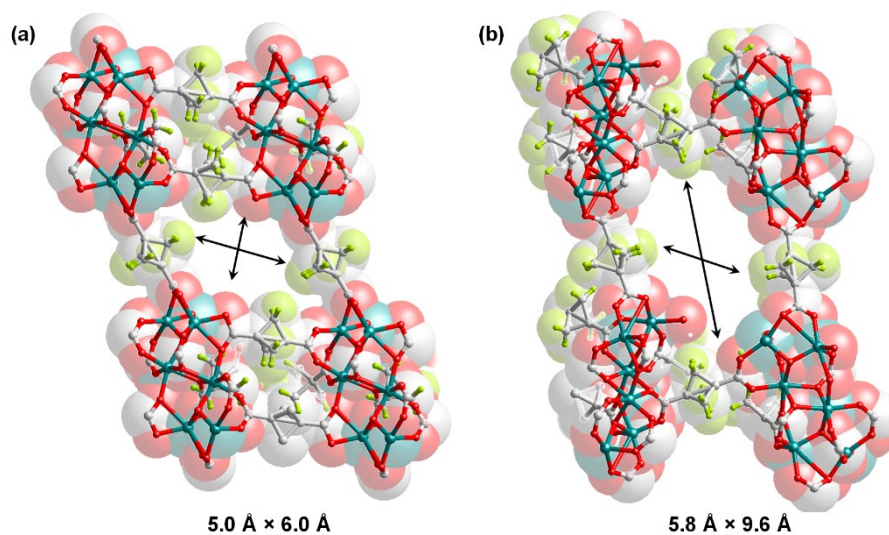
5.0 Å × 6.0 Å   5.8 Å × 9.6 Å

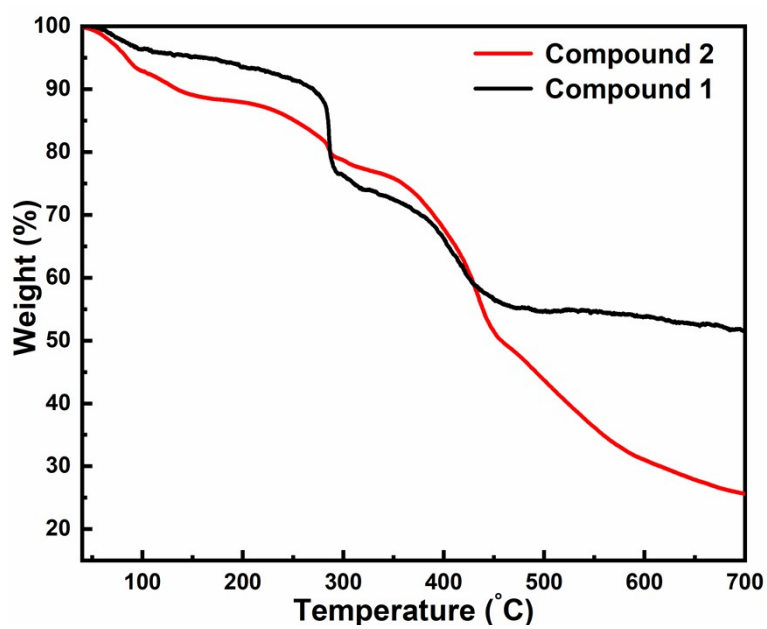**Fig. S5** Aperture illustration of two windows in compound 1.

Fig. S6 TG curves of dichloromethane-changed compound 1 and 2.

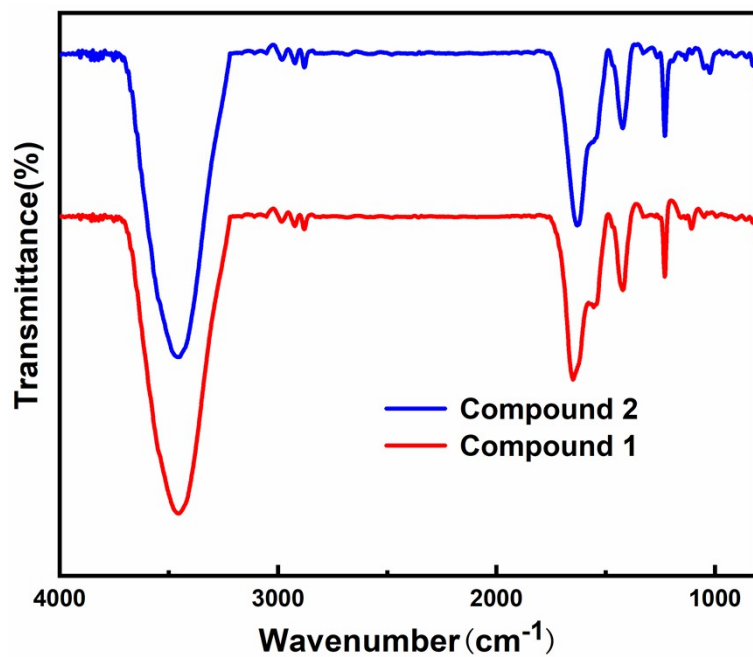**Fig. S7** Fourier transform infrared spectroscopy of as-synthesized compound 1 and compound 2. The strong peak at range of 3000-4000 cm^{-1} should be attributed to large amount of solvents in the cavity of frameworks.
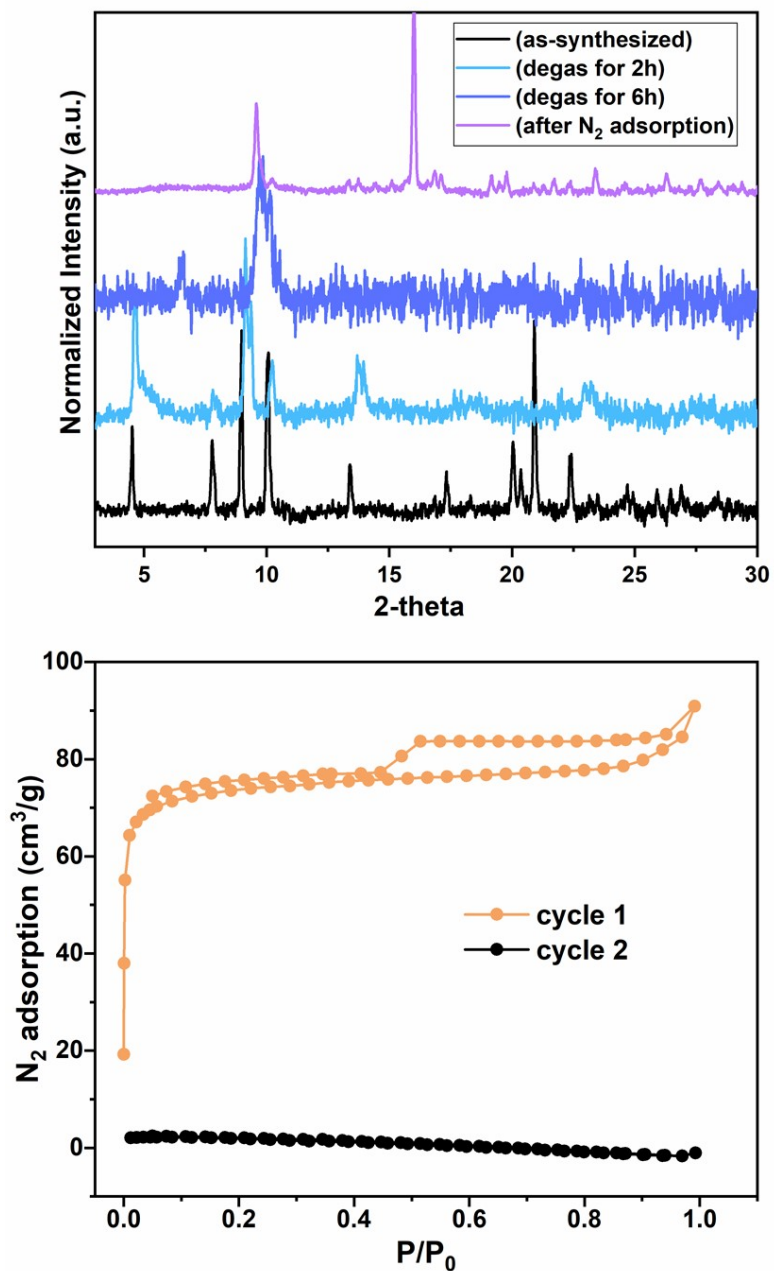
Fig. S8 Comparison of PXRD patterns of compound 2 between the samples of as-synthesized, after degas and after N_2 adsorption (above). Multiple N_2 adsorption experiments on compound 2 at 77 K (below).
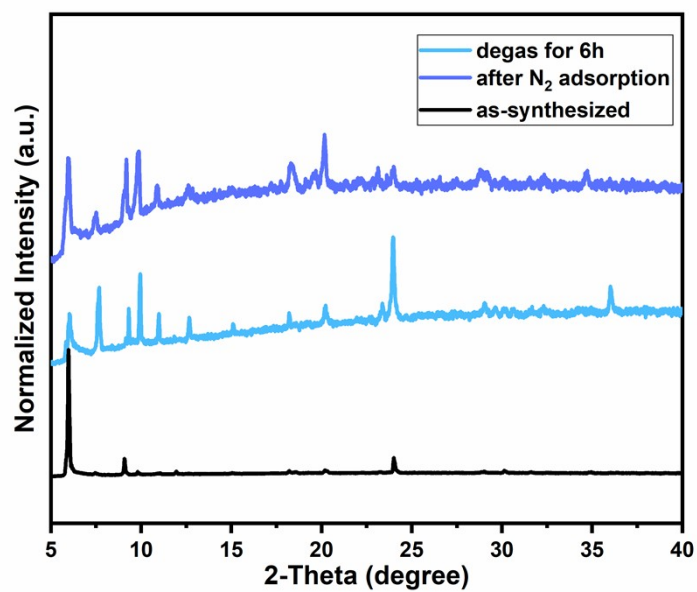
Fig. S9 Comparison of PXRD patterns of compound 1 between the samples of as-synthesized, after degas and after N_2 adsorption.
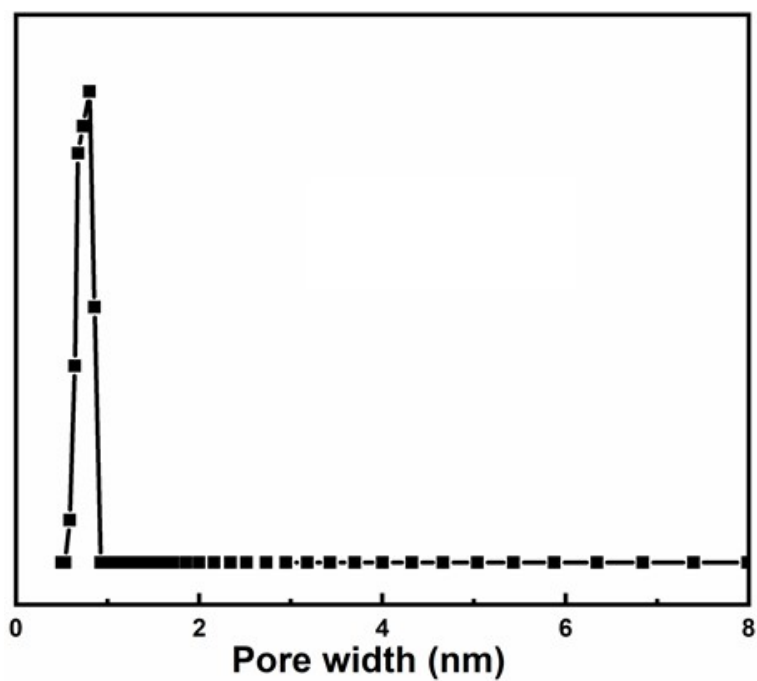

Fig. S10 Pore-size distribution of compound 1 from N_2 adsorption isotherm at 77 K.
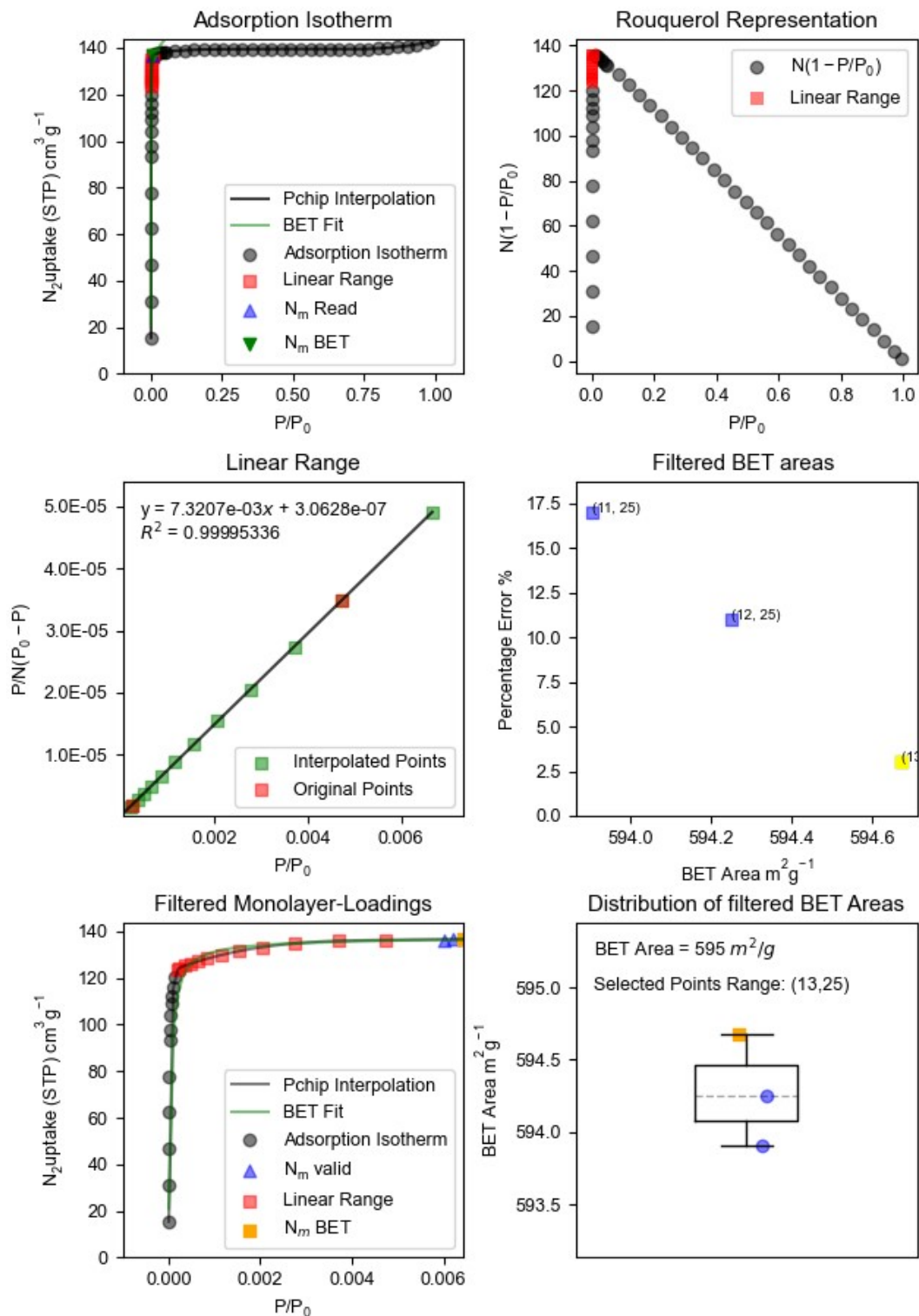
Fig. S11 BETSI analysis for compound 1. (Adsorbate: N_2)

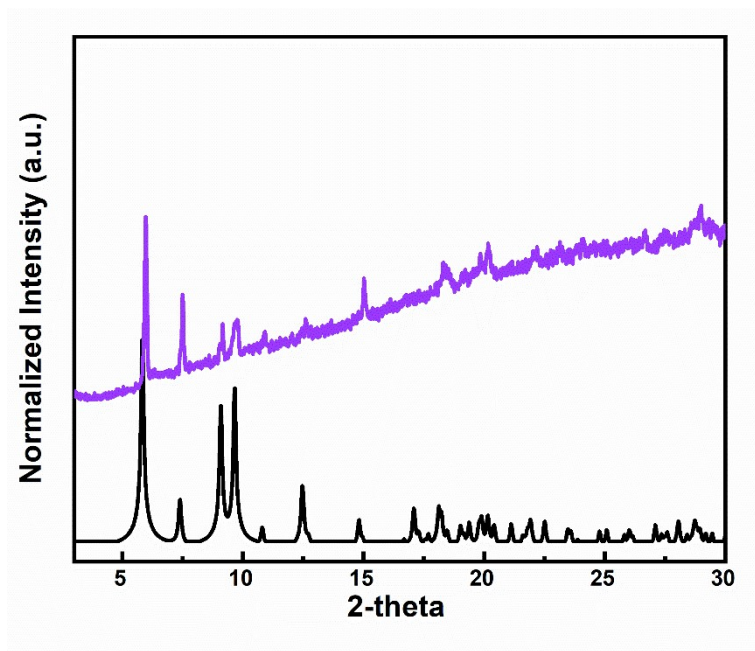**Fig. S12** PXRD patterns of compound 1 after Xe/Kr adsorption measurements.
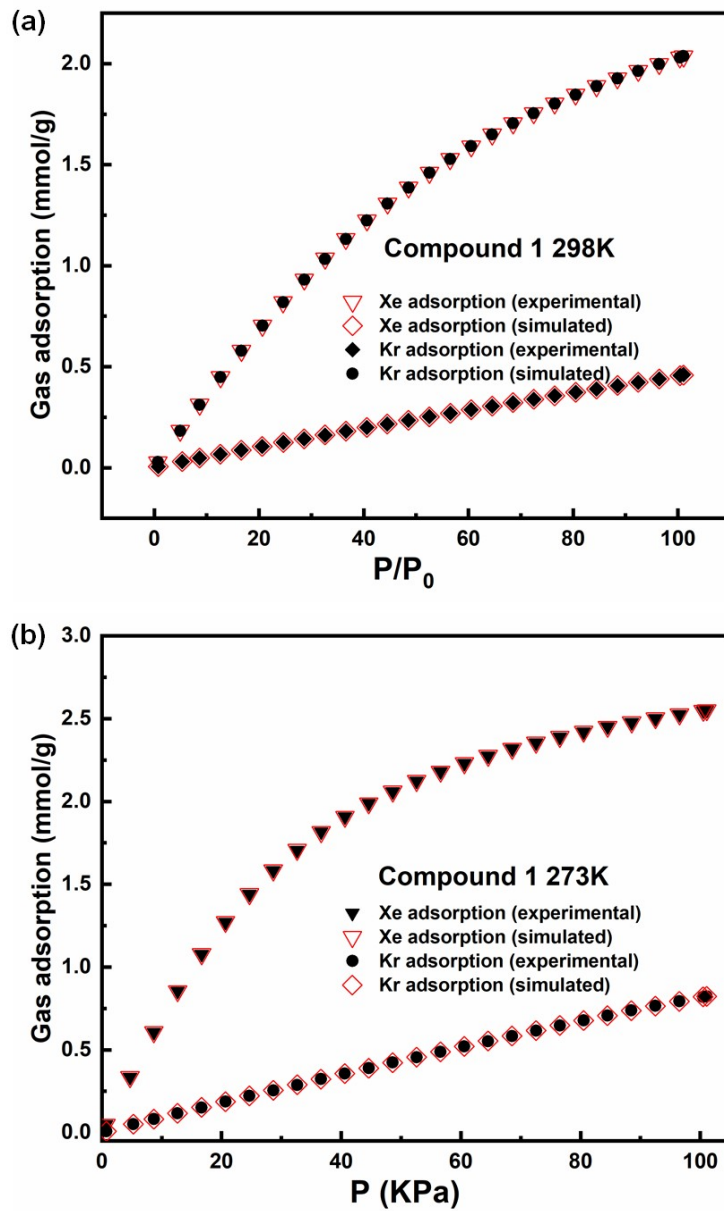
Fig. S13 Fitting graphs of Xe/Kr adsorption isotherms for compound 1 and compound 2 at 298 K (a) and 273 K (b).
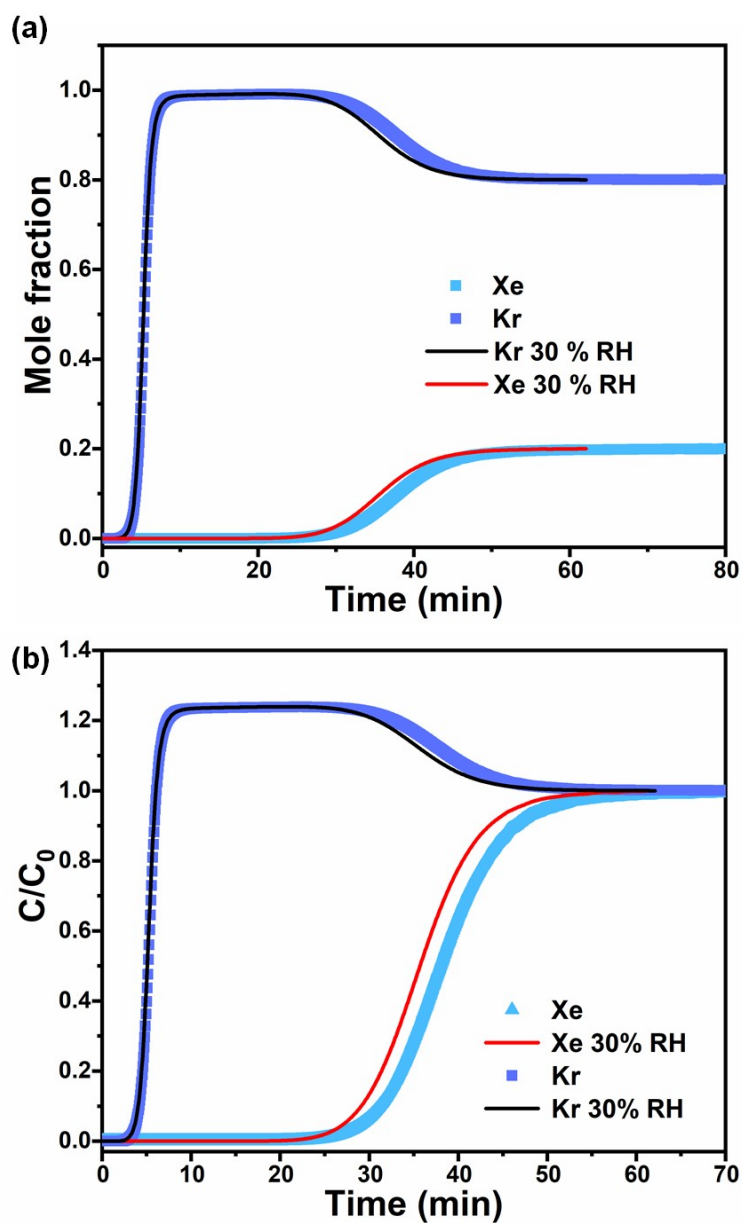
Fig. S14 Experimental breakthrough curves with a step-input of a Xe/Kr mixture (Xe : Kr = 20 : 80) at 298 K under 30 % RH condition (a: outlet Xe/Kr mole ratio; b: outlet concentration/inlet concentration).

Table S1. Crystal data and structure refinement for compound 1.

Identification code	compound 1
Empirical formula	C43 H60 Co6 O31
Formula weight	1482.563
Temperature	296(2) K
Wavelength	0.71073 Å
Crystal system	Monoclinic
Space group	$P2_1/c$
Unit cell dimensions	a = 16.122(18) Å $\alpha = 90°$.
	b = 19.45(2) Å $\beta = 109.994(11)°$.
	c = 11.037(12) Å $\gamma = 90°$.
Volume	3252(6) Å^3
Z	2
Density (calculated)	1.514 mg/m^3
Absorption coefficient	1.579 mm^{-1}
F(000)	1517.549
Theta range for data collection	1.704 to 25.165°.
Index ranges	-19<=h<=19, -23<=k<=20, -13<=l<=13
Reflections collected	17995
Independent reflections	5100 [R(int) = 0.1125]
Completeness to theta = 25.165°	98.1 %
Refinement method	Full-matrix least-squares on F^2
Data / restraints / parameters	5100 / 992 / 335
Goodness-of-fit on F^2	1.0148
Final R indices [I>2sigma(I)]	R1 = 0.0834, wR2 = 0.2082
R indices (all data)	R1 = 0.1311, wR2 = 0.2335
Largest diff. peak and hole	1.4992 and -1.7310 e.Å^{-3}

Table S2.   Crystal data and structure refinement for compound 2.

Identification code	compound 2
Empirical formula	C36.5 H59 Co4 N6 O25
Formula weight	1217.634
Temperature	296(2) K
Wavelength	0.71073 Å
Crystal system	Orthorhombic
Space group	Fmmm
Unit cell dimensions	$a = 17.303(15)$ Å $\quad \alpha = 90°$.
	$b = 39.32(3)$ Å $\quad \beta = 90°$.
	$c = 16.698(15)$ Å $\quad \gamma = 90°$.
Volume	11361(17) Å^3
Z	8
Density (calculated)	1.424 mg/m^3
Absorption coefficient	1.227 mm^{-1}
F(000)	5039.585
Theta range for data collection	1.036 to 22.524°.
Index ranges	-18<=h<=18, -41<=k<=42, -17<=l<=17
Reflections collected	19848
Independent reflections	2030 [R(int) = 0.0810]
Completeness to theta = 22.524°	98.8 %
Refinement method	Full-matrix least-squares on F^2
Data / restraints / parameters	2030 / 163 / 141
Goodness-of-fit on F^2	1.0455
Final R indices [I>2sigma(I)]	R1 = 0.0754, wR2 = 0.2182
R indices (all data)	R1 = 0.0888, wR2 = 0.2283
Largest diff. peak and hole	1.5952 and -1.0121 e.Å^{-3}

Table S3. Element analysis results for compound 1 and compound 2.

Elements (wt.)	C (%)	H (%)	O (%)	N (%)
Calculated for 1	35.20	3.04	32.15	0
Experimental for 1	34.46	3.27	33.54	0
Calculated for 2	37.20	3.31	29.15	1.70
Experimental for 2	36.18	3.66	27.43	1.25

023_ALERT_3_A Resolution (too) Low [sin(theta)/Lambda < 0.6].. 0.54 Ang^{-1}

341_ALERT_3_B Low Bond Precision on C-C Bonds .... 0.018 Ang.

Response: A full set of data of compound 2 was collected, but the very high angle data was dominated by noise. It's difficult to harvest high angle diffraction points due to the weak diffraction capability, even when measured over a long time. In addition, compound 2 has poor structural stability and crystallinity. It cannot maintain its pristine crystallinity in the long time measurement. To improve the data quality, we cut off the bad diffraction points at high resolution.